https://dx.doi.org/10.22161/ijaers.5.2.16 ISSN: 2349-6495(P) | 2456-1908(O)

Speed and Current Limiting Control Strategies for BLDC Motor Drive System: A Comparative Study

Adel A. Obed[1], Abbas K. Kadhim[2]

[1]Assist. Prof. Dr., Department of Electrical Power Engineering Techniques, Electrical Engineering Technical College, Middle Technical University, Baghdad, Iraq

[2]MSc.Student, Department of Electrical Power Engineering Techniques, Electrical Engineering Technical College, Middle Technical University, Baghdad, Iraq

Abstract*—As a result of increasing the use of the brushless direct current (BLDC) motor in many life applications instead of the traditional motors, it is important to list and specify the more for its controlling methods. This paper presents a number of speed and current controlling methods as hysteresis band, variable dc-link bus voltage and pulse width modulation (PWM) controlling methods. These controlling methods have proportional integral derivative (PID) gains which are optimized by using particle swarm optimization (PSO) algorithm. By using fast Fourier transform (FFT) analysis to study the controller behavior from frequency analysis of the output signals and compute total harmonic distortion (THD), it can specify the more useful controlling method. The framework is modeled and fabricated by using Matlab/Simulink.*

Keywords*—*BLDC Motor Drive Model, FFT Analysis, Mathematical Representations, Matlab/Simulink, PSO Algorithm.

I. INTRODUCTION

The BLDC motor applications turn into most requests and the rapid rising such as aerospace, automotive, office automation, household appliances and different industries. It has important advantages like, long operation life, noiseless operation, high efficiency, high dynamic response, wide speed range, low temperature and can withstand vibrations and shock, this will get better stability of the drive [1,2]. BLDC motors are really a type of permanent magnet synchronous motors in spite of its name. The commutation of the currents is done by electronically switches inverter which is driven by a DC power supply. The commutations are resolved by rotor position; this is detected either by sensorless mechanisms or position sensor. This motor type is consisting of permanent magnets in the rotor and three phase publicized windings in the stator that are wound as trapezoidal b-emfs. The induced currents in the rotor can be lapsed due to the high resistivity of both stainless steel and magnet. No damper windings are modeled because they will reduce the magnetic force [3]. The stator current must be semi-square in order to synchronize with b-emfs to make stable and higher torque at steady speed. The operation of this motor is done when two phases are ON state and the third is floating for every 60 electrical degrees [4-6].

Different simulation models are done by many searchers to anatomize the behavior and operation of the arrangement to give the accurate torque rate that is identifying with current and b-emfscorresponding to suitable set point speed, they work on tuning PID parameters as based on Ziegler-Nicholas, genetic algorithm tuning methods and other work on adjusting PID parameters by fuzzy optimized algorithm or using fractional order PID controller and PID controller with two degrees of freedom [7-13].

Speed control of BLDC motor takes a necessary role in the modern control. In this paper, different control strategies; hysteresis band control, variable dc-link control and PWM control are performed and tested on the BLDC motor and their PID gains are obtained by PSO algorithm using MATLAB software program. The different controlling methods are tested and the results are compared and discussed. Finally, the frequency analysis for the motor current is implemented using FFT analysis and the THD is also computed to study the effect of controlling methods.

II. MATHEMATICAL MODEL OF BLDC MOTOR

BLDC motor modeling cans appear in the parallel attitude as a synchronous machine with three-phase windings. As any model multi-phase motors, one style of them is fed by three-phase voltage source as a BLDC motor is as shown in Fig. 1. The peak voltage must not to be overtaken the

https://dx.doi.org/10.22161/ijaers.5.2.16 *ISSN: 2349-6495(P) | 2456-1908(O)*

ultimate voltage frontier of the motor and not to be lower than the back-emf induced voltage [14, 15].

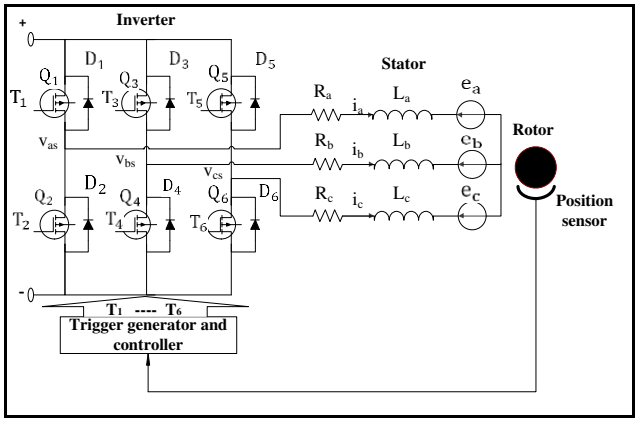

Fig. 1: Three-phase BLDC motor equivalent circuit.

Based on Kirchhoff's voltage law the matrix shape of the phase voltage equations of the BLDC motor can be extracted as:

$$\begin{bmatrix} v_{as} \\ v_{bs} \\ v_{cs} \end{bmatrix} = \begin{bmatrix} R & 0 & 0 \\ 0 & R & 0 \\ 0 & 0 & R \end{bmatrix} \begin{bmatrix} i_a \\ i_b \\ i_c \end{bmatrix} + \begin{bmatrix} L-M & 0 & 0 \\ 0 & L-M & 0 \\ 0 & 0 & L-M \end{bmatrix} \frac{d}{dt} \begin{bmatrix} i_a \\ i_b \\ i_c \end{bmatrix} + \begin{bmatrix} e_a \\ e_b \\ e_c \end{bmatrix} \quad \ldots\ldots (1)$$

where v_{as},v_{bs} and v_{cs} are the stator voltages; R is the per phase stator resistance, it has assumed to be equal for all windings; i_a, i_b and i_c are the stator phase currents and e_a, e_b and e_c are the back-emf 's phase voltage.

By subtraction calculations of the phase voltages equations the line voltage equation can be obtained as [12, 14]:

$$\begin{bmatrix} v_{ab} \\ v_{bc} \\ v_{ca} \end{bmatrix} = \begin{bmatrix} R & -R & 0 \\ 0 & R & -R \\ -R & 0 & R \end{bmatrix} \begin{bmatrix} i_a \\ i_b \\ i_c \end{bmatrix} + \begin{bmatrix} L-M & M-L & 0 \\ 0 & L-M & M-L \\ M-L & 0 & L-M \end{bmatrix} \frac{d}{dt} \begin{bmatrix} i_a \\ i_b \\ i_c \end{bmatrix} + \begin{bmatrix} e_a - e_b \\ e_b - e_c \\ e_c - e_a \end{bmatrix} \quad \ldots\ldots\ldots (2)$$

Since each voltage equation is a linear combination of the other two voltages equations. So that only two equations are needed for simplifying the later construction system model. By disposal away one equation and ignoring one variable using the following balance relationship:

$i_a+i_b+i_c=0$ …… (3)

Then from above equations can modify the following equations:

$$\frac{d}{dt} i_a = -\frac{R}{L-M} i_a + \frac{2}{3(L-M)} (v_{ab} - e_{ab}) + \frac{1}{3(L-M)} (v_{bc} - e_{bc}) \ldots\ldots\ldots\ldots (4)$$

$$\frac{d}{dt} i_b = -\frac{R}{L-M} i_b - \frac{1}{3(L-M)} (v_{ab} - e_{ab}) + \frac{1}{3(L-M)} (v_{bc} - e_{bc}) \ldots\ldots\ldots\ldots (5)$$

The trapezoidal back-emfs are related to a function of rotor position. It has 120° phase shift, so the equation of each phase can be expressed as [2, 14]:

$$e_a = \frac{k_e}{2} w_m F(\theta_e) \ldots\ldots\ldots\ldots (6)$$

$$e_b = \frac{k_e}{2} w_m F(\theta_e - \tfrac{2\pi}{3}) \ldots\ldots\ldots\ldots (7)$$

$$e_c = \frac{k_e}{2} w_m F(\theta_e + \tfrac{2\pi}{3}) \ldots\ldots\ldots\ldots (8)$$

where k_e is the back-emf constant; w_m is the rotor speed and θ_e is electrical rotor angle which is equal to:

$$\theta_e = \frac{p}{2} \theta_m \ldots\ldots\ldots\ldots (9)$$

where p is the number of poles and θ_m is the mechanical rotor angle which is equal to:

$$\theta_m = \int_0^t w_m \, dt \ldots\ldots\ldots\ldots (10)$$

The function $F(\theta_e)$ gives the trapezoid waveform of the back-emf, the function can be written for one period as:

$$F(\theta_e) = \begin{cases} 1 & 0 \le \theta_e < \frac{2\pi}{3} \\ 1 - \frac{6}{\pi}(\theta_e - \frac{2\pi}{3}) & \frac{2\pi}{3} \le \theta_e < \pi \\ -1 & \pi \le \theta_e < \frac{5\pi}{3} \\ -1 + \frac{6}{\pi}(\theta_e - \frac{5\pi}{3}) & \frac{5\pi}{3} \le \theta_e < 2\pi \end{cases} \ldots\ldots\ldots (11)$$

Based on Newton's 2nd law and identical to the DC motor, the anatomy of BLDC motor power and torque can be accomplished from the energy transfer standpoint, the generality of the power is transferred by the torque effect to the rotor through the air-gap which is pleaded the electromagnetic power as[16]:

$$p_e = e_a i_a + e_b i_b + e_c i_c \ldots\ldots\ldots\ldots (12)$$

By eliminated the stray and mechanical losses; the electromagnetic power is completely converted to kinetic energy so [17]:

$$p_e = T_e w_m \ldots\ldots\ldots\ldots (13)$$

where T_e is the electromagnetic torque, so that from equations (6-8, 12 and 13) the electromagnetic torque can be extracted as:

$$T_e = \frac{k_t}{2} [F(\theta_e) i_a + F(\theta_e - \tfrac{2\pi}{3}) i_b + F(\theta_e + \tfrac{2\pi}{3}) i_c] \ldots\ldots (14)$$

And the motion equation has to be included as:

$$T_e - T_L = J \frac{dw_m}{dt} + k_f w_m \ldots\ldots\ldots\ldots (15)$$

where T_L is the load torque, k_t is the torque constant, k_f is the viscous friction constant and J is the rotor moment of inertia.

III. SPEED CONTROL STRATEGIES OF BLDC MOTOR

Comparing with other motor types, the BLDC motor has more intricate control algorithm. There are three general methods to control the speed of BLDC motor as mentioned before. Typically, dual-closed-loop speed control is common in control system. The inner loop is used to adjust the current as well as the torque to the suitable value, while the outer loop is the speed loop,

https://dx.doi.org/10.22161/ijaers.5.2.16 *ISSN: 2349-6495(P) | 2456-1908(O)*

that's used to control the motor speed. The speed controller is a portion of a closed-loop control that the actual speed is measured and draw an analogy with the set-point speed to find the error speed which its treatment by the controller to provide the better signal to the plant to obtain the measured speed as more closed to the set-point speed.

3.1 **Hysteresis Band Speed Control Method**

This is the simplest closed-loop control method, where the amount of the controlled speed is forced to pause within a certain limit (hysteresis band) around a set-point amount. Fig. 2 shows the schematic diagram of the BLDC motor hysteresis band speed control. As to control the speed of the motor, the motor will turn-off if the speed arrives at a certain level over the set-point speed and back turn-on when the speed declines below a certain level below the set-point speed [2, 18].

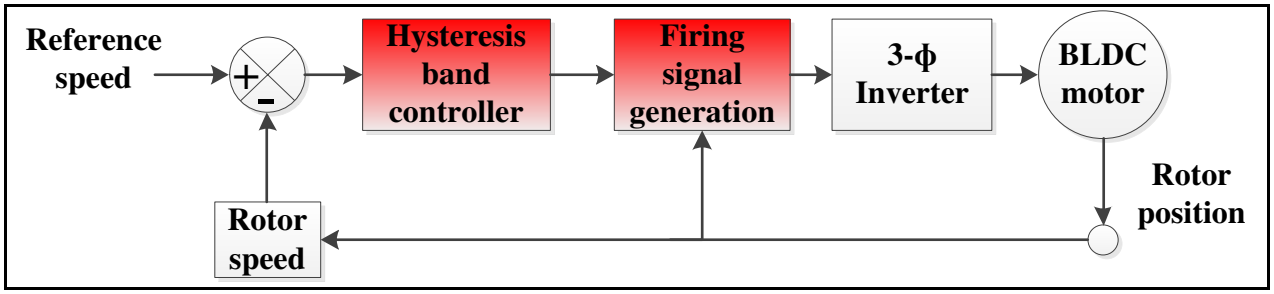

Fig.2: Schematic diagram of the BLDC motor drive hysteresis band speed control system.

3.2 **Variable DC-Link Voltage Speed Control Method**

By this method, the control of the DC bus voltage is used for obtaining the controlling speed. The motor voltage variation can be achieved by changing the PWM duty cycle signal of the voltage controller (DC-DC converter) [19]. The buck converter connection is used here which is converting the fixed voltage into a mutable voltage to confirm the required speed of the BLDC motor speed control drive. Fig. 3 shows the schematic diagram of the BLDC motor drive variable dc-link speed control system. The rotor speed is subtracted from reference speed and the error signal is fed to the speed controller that its output is limited by the reference current. The value of the reference current is derived from the reference torque by the following relationship [2]:

$$I_{ref} = \frac{T_{ref}}{k_t} \quad \text{..... (16)}$$

The equivalent signal of the DC-link current is synthesized from the three-phase stator currents then subtracted from the speed controller output. After that, the error signal is fed to the torque controller. The output signal from the torque controller is limited by an applied voltage source. Then the final control signal is supplied to the DC-DC converter to control the duty cycle using PWM technique by comparing it to the triangular wave which will give the voltage amplitude required to the inverter to maintain the desired speed.

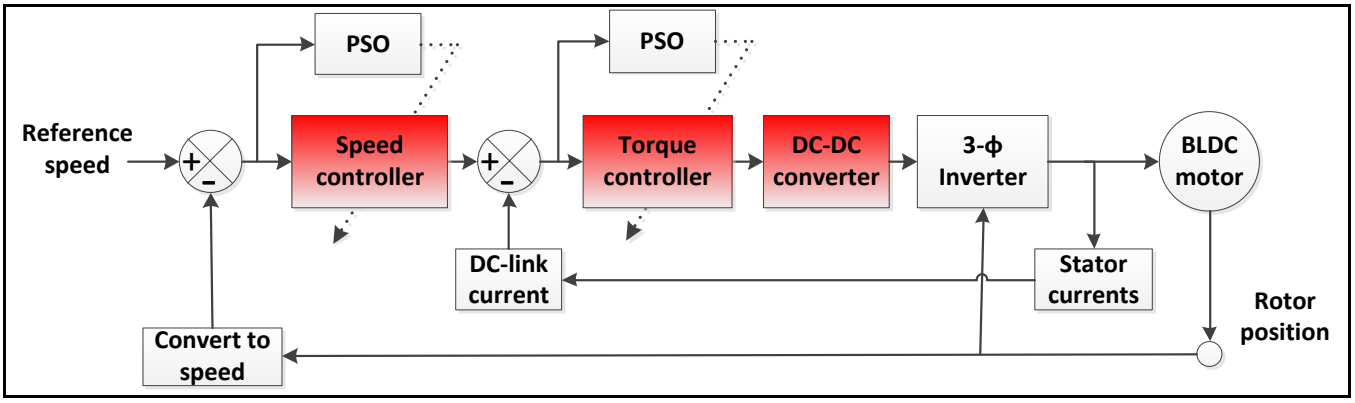

Fig.3: Schematic diagram of the BLDC motor drive variable dc-link voltage speed control system.

3.3PWM Speed Control Method

The schematic block diagram of the command system used in this method is same as that in Fig. 3 but the DC-DC converter block is replaced by the Pulse Width Modulation (PWM) block not to modify the dc bus voltage but to modify the duty cycle of switches firing signals as shown in Fig. 4. The BLDC motor speed directly changes by modulation the duty cycle of the inverter switches firing signals depends on the control error. In this control method, the motor will turn on and

https://dx.doi.org/10.22161/ijaers.5.2.16 *ISSN: 2349-6495(P) | 2456-1908(O)*

off at a high rate, the chopping frequency is fixed but the control error will change the duty cycle's length [2]. The truth that the frequency is fixed lets that the electromagnetic noise and acoustic filtering easier. The switching frequency is usually 20-50 KHz where the higher frequency will give low variation in current and also smoother torque. The suggest control system consists of proposed currents sensors to apply the necessary three phase currents to obtain dc link current. This is useful for retaining the motor current at the desired value at starting and step change speed by presence the torque controller. By this method, the control of the firing signals duty cycle length of a PWM; obtaining a controlling speed. Here the torque controller output is fed to the PWM block to compare it with the triangular waveform where the output of the comparator is a low or high signal which turns as a chopping signal for the inverter.

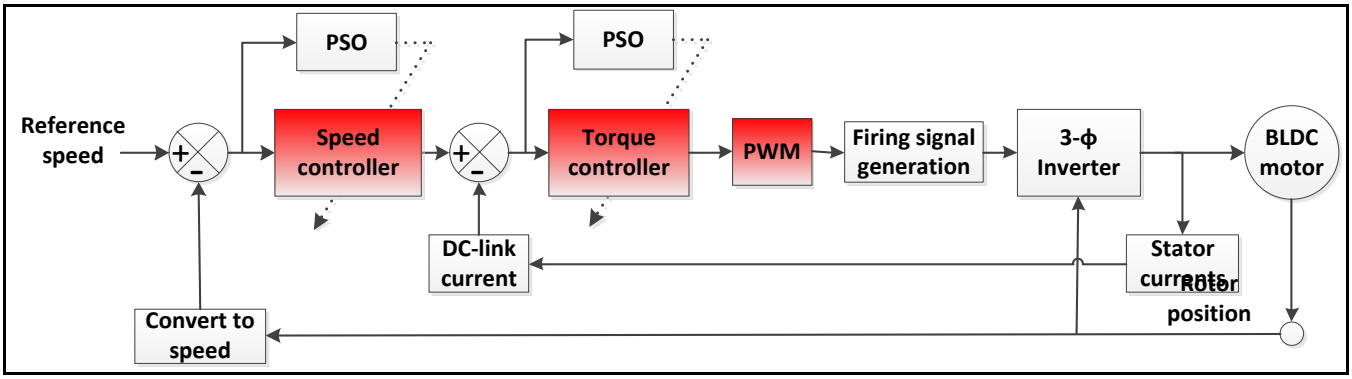

Fig. 4: Schematic diagram of the BLDC motor drive PWM speed control system.

IV. EMPLOYMENT OF PARTICLE SWARM OPTIMIZATION FOR BLDC MOTOR CONTROL SYSTEM

Particle Swarm Optimization (PSO) is an investigative algorithm first come in 1995 as a mohair amount by Russell Eberhart and James Kennedy [20]. They look that the bees swarm will job altogether to detect an area with ultimate food. Each demarcation bee in the swarm seeking a casual area and gets the area for the ultimate plenty food. The demarcation bee will then pass this location to the whole swarm then compare this demarcation position of food among the other positions informed by the other bees. Eberhart and Kennedy convert the biological notions of the swarm attitude to engineering converge by using the nature idea; a swarm will find the better solution from the swarm intelligence [21].

In the engineering systems, the particles in the swarm are demarcation elements in the swarm accountable for moving to their personal best values (pbest) and the swarm (global) best value (gbest) all the however continually seeking their current position to observe for good values than what the block has. The blocks' position is the location given a particular border for which to seek in it. Estimation of the position is completed during a fitness function that responds the optimal solution. The basic PSO algorithm is below as described in the flowchart that is shown in Fig. 5 [22-24]. For PID controller system, there always four fitness functions to depict the system response which are Integrated Square of Error (ISE), Integrated Absolute Error (IAE), Integrated Absolute Time weight Error (IATE) and Integrated of Time weight Square Error (ITSE). They are used to minimize the steady-state error, maximum overshoot, reference tracking error, settling time and rise time for the PSO-PID controller system. Here, is used multi-fitness functions based on the (ISE) and overshoot (Mp) criterions as follow:

Function for Fitness = min (ISE) + min (Mp) …… (17)

where:

$ISE = \int e^2(t)\, dt$…… (18)

$Mp = \max(n) - (n_{ref})$ …… (19)

$e(t) = n(t) - n_{ref}(t)$ …… (20)

where n(t) is the output speed of the model and $n_{ref}(t)$ is the desired speed.

Equations (21-22) shows the updating of velocity $v_i(t)$ and the current position $x_i(t)$ respectively for each swarm particle. Then the main loop and the fitness function begin to perform their calculations for updating the position of particles. If the new amount is superior to the previous lbest then the new amount is adjusted to lbest. Compatible, gbest amount is also updated as the better lbest. The velocity of any rep can be adjusted by the equation:

$$v_i^{k+1} = W * v_i^k + C_1 * R_1 * (lbest_i - x_i^k) + C_2 * R_2 * (gbest_i - x_i^k) \quad \text{…… (21)}$$

and the current position can be adjusted by the equation:

$$x_i^{k+1} = x_i^k + v_i^{k+1} \quad \text{…… (22)}$$

where v_i^k is the velocity at iteration k of particle i, x_i^k is the current position at iteration k of particle i, W is the weight of inertia which can be represented by equation (3.7) below, C_1, C_2 are positive constants of acceleration, R_1

https://dx.doi.org/10.22161/ijaers.5.2.16 *ISSN: 2349-6495(P) | 2456-1908(O)*

and R_2 are casual variables uniformly extend in range (0-1).

$$W = W_{max} - \left(\frac{W_{max}-W_{min}}{k_{max}}\right) * k \quad \text{..... (23)}$$

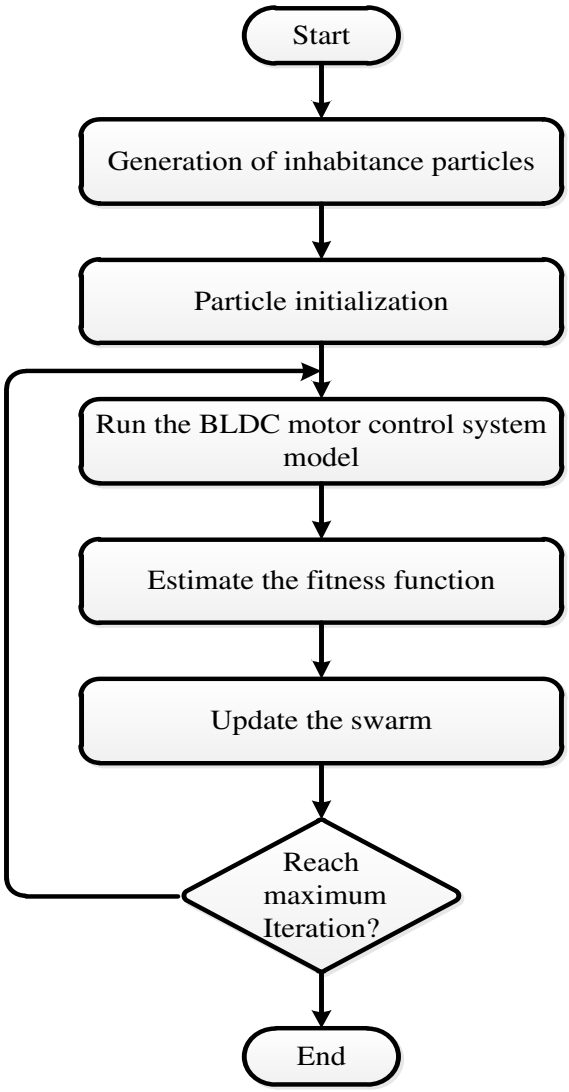

Fig. 5: The general flowchart of PSO.

If the predetermined maximum iteration number is reached, then stop the algorithm. Otherwise, do another initialization for any particle and repeat the operation.

The PSO algorithm is performed in MATLAB with its parameters shown in Table 1. Among Linear Quadratic Regulator (LQR) and Genetic Algorithm (GA) methods, PSO algorithm is greater efficient to get better the characteristics of step response as reducing the rise time, steady-state error, settling time and maximum overshoot and undershoot for controlling the speed [25].

Table.1: PSO parameters values.

PSO-Parameters	Values
Size of the swarm (no. of bees)	50
Maximum iteration number (k_{max})	50
Dimension	3
C_1	1.2
C_2	1.2
W_{max}	0.9
W_{min}	0.01

V. SIMULATION AND RESULTS

The plenary BLDC motor drive Simulink model has been performed using MATLAB/SIMULINK software. Each part of the BLDC motor drive model is finalized by a set of mathematical model. As a set of equations (1-15) for the motor block when combined together outline the complete system model as shown in Fig. 5. The motor parameters used here are shown in Table 2.

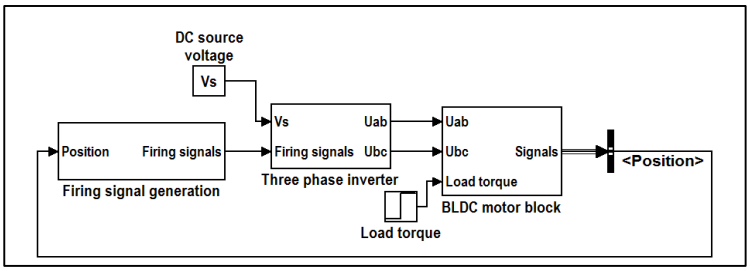

Fig. 6: Simulink model of BLDC motor drive system.

Table.2: Data of BLDC motor.

Parameters types	Parameters values	Units
Rated power	1200	W
Rated voltage	76	V
Rated current	16	A
Rated torque	2.9	N.m
No load current	0.66	A
No load speed	3500	rpm
Torque constant	0.207	Nm/A
Voltage constant	0.207	V.s/rad
Terminal resistance	0.110	Ω
Inductance(L-M)	0.6	mH
Viscous damping factor	$1.3x10^{-4}$	N.m s/rad
Rotor inertia	$1.7x110^{-3}$	$kg.m^2$
Number of poles	8	

Fig. 7 shows the simulink model of BLDC motor drive with hysteresis band speed controller block. The rotor speed is fed to the relay block and the set-point speed

https://dx.doi.org/10.22161/ijaers.5.2.16 *ISSN: 2349-6495(P) | 2456-1908(O)*

value is the input to the relay block upper and lower limits plus and minus half of the hysteresis bandwidth respectively. The width of the hysteresis band is 1.2% of the set-point speed. Fig. 8 shows the rotor speed through a set-point of 2500 rpm and the load torque 2.9 N.m is applied at 0.5 seconds. The speed stays within the hysteresis band of ±30rpm around the set-point speed. The electromagnetic torque and phase current i_a are shown in Figs. 9 and 10 respectively.

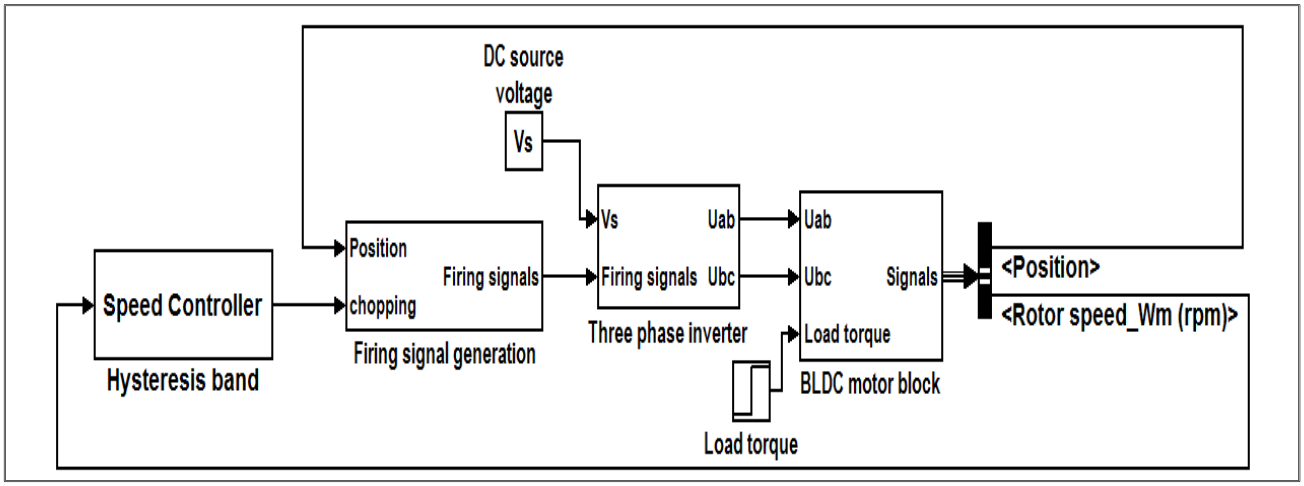

Fig. 7: Simulink model of BLDC motor drive with hysteresis band speed controller.

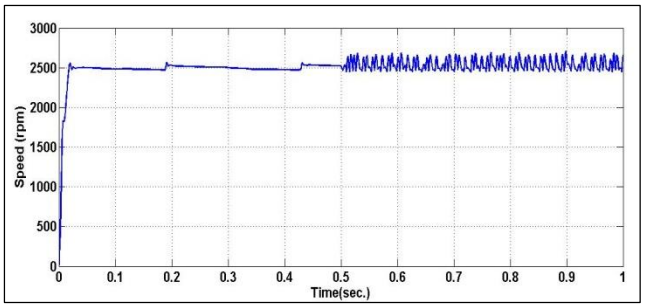

Fig. 8: BLDC motor speed using hysteresis band control.

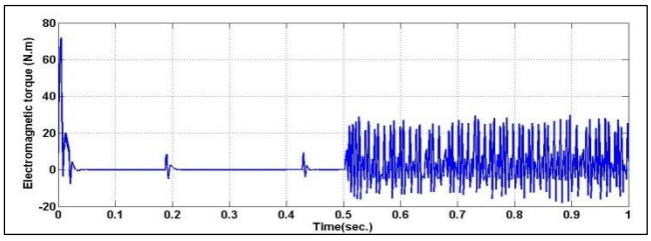

Fig. 9: BLDC motor electromagnetic torque using hysteresis band control.

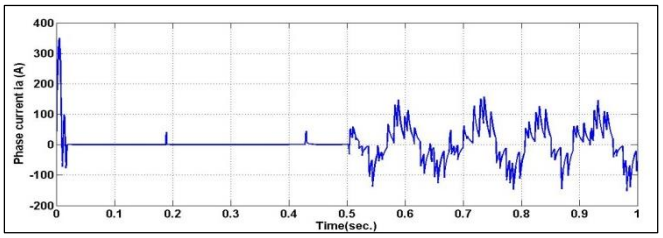

Fig. 10: BLDC motor phase current using hysteresis band control.

The BLDC motor Simulink model based on dual closed loop for speed and current limiting control using PID controllers and controlled DC bus voltage has been enforced using MATLAB/SIMULINK software (R2015a) with Bogaki-Shampine (ode3) fixed step type solver by fundamental sample time is $3*10^{-6}$ seconds as shown in Fig. 11. The dual control loops are used; where the outer loop is used to control the rotor speed and the inner loop to control currents or torque. The PID controllers' gains are optimized using PSO algorithm.After iteration 37, the gains are shown in Table 3.

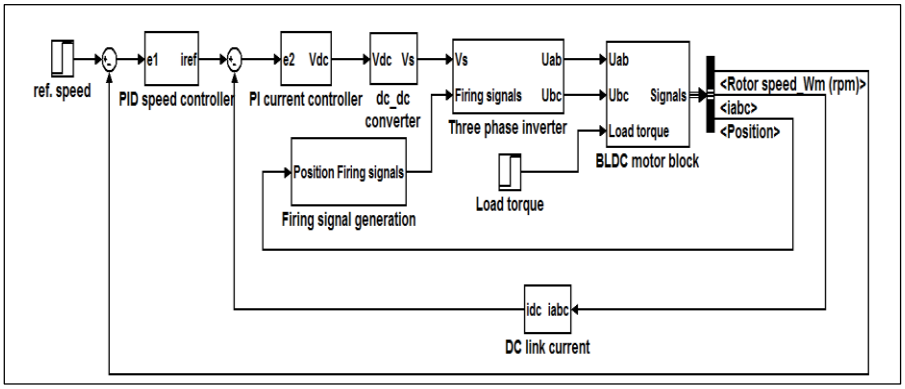

Fig.11: Simulink model of BLDC motor drive with variable DC bus voltage dual loop PID controller

https://dx.doi.org/10.22161/ijaers.5.2.16 ISSN: 2349-6495(P) | 2456-1908(O)

Table.3: PID optimized parameters.

Parameters	Values
Speed controller	
Proportional (k_p)	2.779
Integral (k_i)	0.9898
Derivative (k_d)	0.03751
Current controller	
Proportional (k_p)	2.996
Integral (k_i)	1.391

Fig. 12 shows the speed response for 2000 rpm reference speed starting with no load and the full load 2.9N.m is applied at 0.5 seconds.The electromagnetic torque and phase current i_a are shown in Figs. 13 and 14 respectively. The variable DC link voltage controlling method has some merits. A linear power stage is cheaper but at high current and low voltage, the losses can be high.

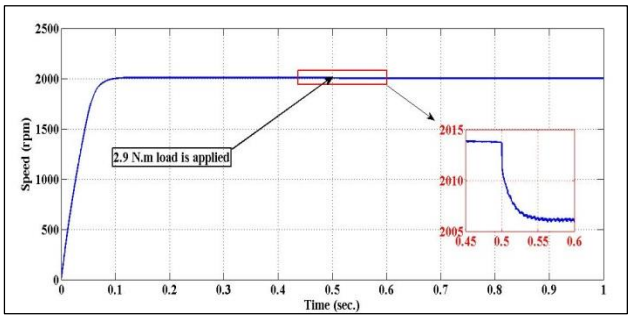

Fig.12: Speed response for variable DC link controller.

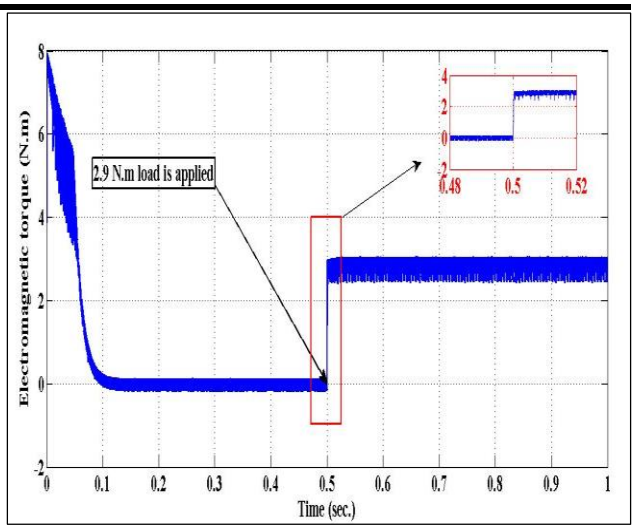

Fig. 13: Electromagnetic torque for the variable DC link controller

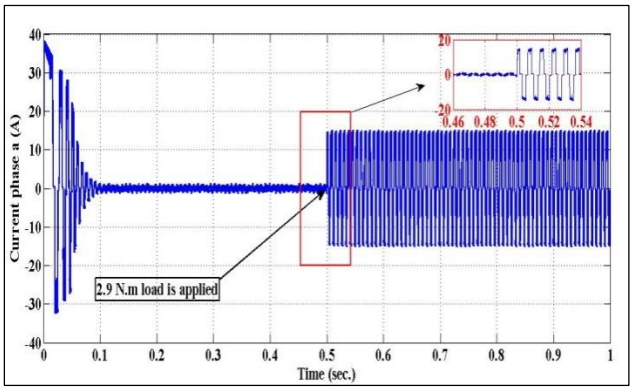

Fig. 14: Current phase (a) for the variable DC link controller.

PWM's technique with the same details in the previous controlling method is shown in Fig. 15. The gains of PID speed controller and PI current controller blocks diagrams are same as that used in the variable DC link control.

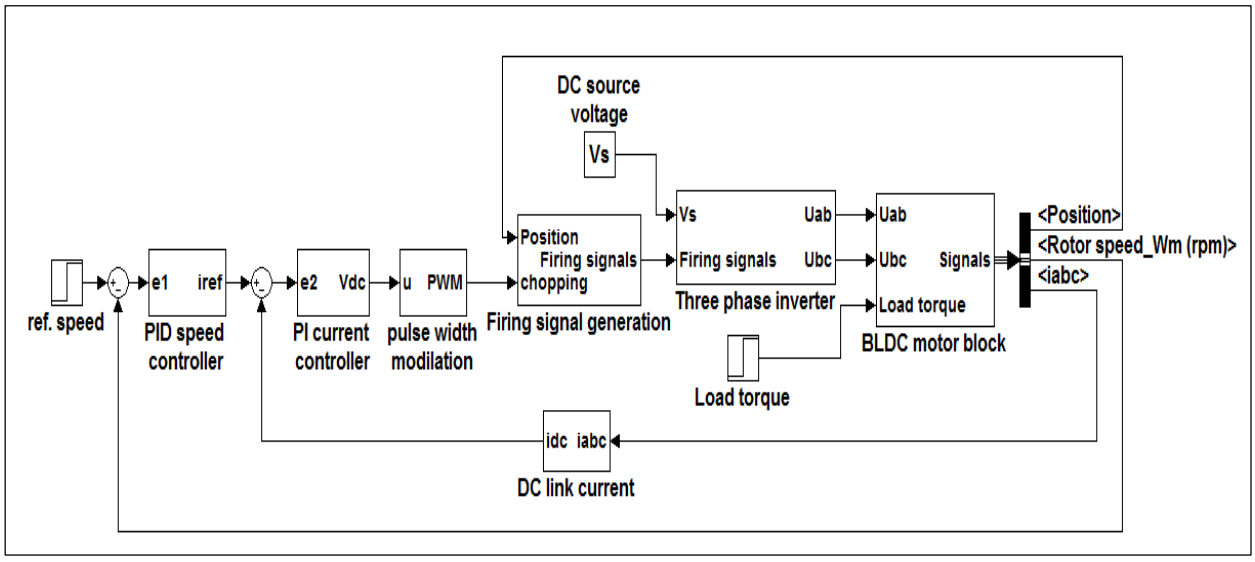

Fig. 15: Simulink model for BLDC motor drive with PWM dual loop PID controller.

https://dx.doi.org/10.22161/ijaers.5.2.16 *ISSN: 2349-6495(P) | 2456-1908(O)*

Fig. 16 shows the speed response for 2000 rpm reference speed starting with no load and the full load 2.9N.m is applied at 0.5 seconds.The electromagnetic torque and phase current i_a are shown in Figs. 17 and 18 respectively.

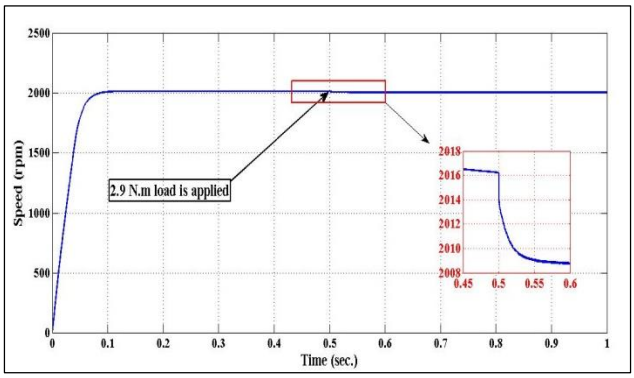

Fig. 16: Speed response for PWM controller.

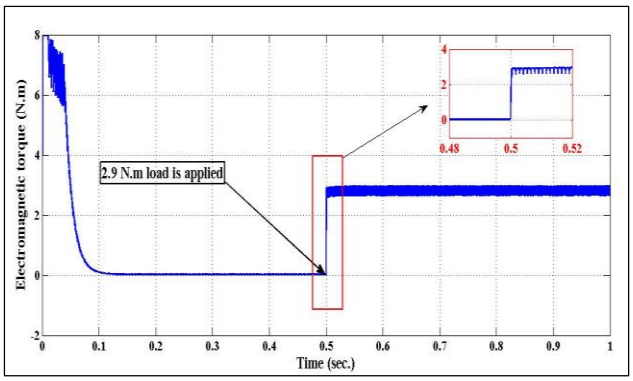

Fig. 17: Electromagnetic torque for PWM controller.

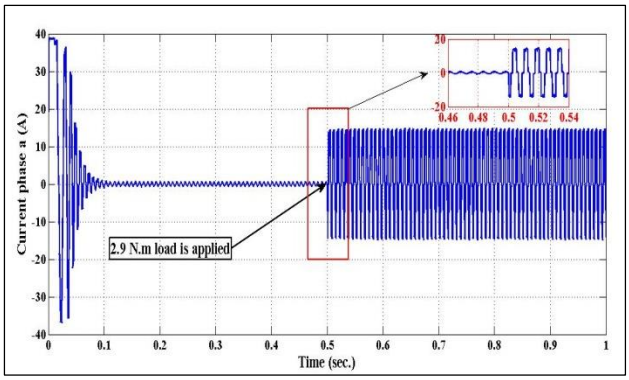

Fig. 18: Current phase (a) for PWM controller.

VI. FREQUENCY ANALYSIS

The current frequency spectrum is a significant factor in the electrical systems. The BLDC motor is nonlinear load has non-sinusoidal current and voltage waveforms, which will produce harmonics in the power line system. Harmonic is a periodic wave component having an integral multiple of the fundamental frequency. Harmonic distortion is a dirty power particular type usually linked with industrial plants that used adaptable power supplies, speed drives, and other equipment's use solid-state switching[2, 26].

The harmonic distortion level of current or voltage can be extracted by the total harmonicdistortion (THD) term of voltage or current waveform as[27]:

$$x_{THD} = \frac{\sqrt{x_2^2+x_3^2+\cdots+x_n^2}}{x_1} \quad \ldots\ldots\ldots\ldots\ldots\ldots\ldots\ldots\ldots\ldots \quad (24)$$

where x is any of current or voltage, x_1 is fundamental value and x_n (n = 1, 2, 3, … etc.) is the harmonics values. Harmonic distortion of voltage and current have existed together (current harmonic distortion causes voltage harmonic distortion). Harmonic distortion increase voltage peaks that make extra stress on motor and wire insulation leads to breakdown and failure. Over and above, harmonics increase RMS current, leads to increase operating temperature of the motor so reducing its life. Many methods are found to identify the harmonics. In this paper, Fast Fourier Transform (FFT) analysis is used because of quick response and easy in implementation [26, 27].

Figs. 19 and 20 show the hysteresis band control phase current $i_a$frequency spectrum at no load and full load respectively. The fundamental frequency is 8Hz and THD is 569.14% for no-load while fundamental frequency is 10Hz and THD is 57.96% for a full load. It is clear that the switching frequency varies with varying load and the harmonics of the fundamental frequency are quite strong which are the main disadvantage of hysteresis control because it makes difficult to filter out the undesired harmonics.Figs.21 and 22 show the same frequency spectrum as the previous conditions but now for variable dc-link control. The figures show that the frequency content is constant at no load and full load by 125Hz and THD is 62.69% at no load and 33.16% at full load.Figs. 23 and 24 show the same frequency spectrum as the previous conditions but now for PWM control. The fundamental frequency is also constant 125Hz and independent on the varied load but here the THD is 8.94% at no load and 28.49% at full load for that this method is more popular than the other two methods as filtering becomes more easier.

https://dx.doi.org/10.22161/ijaers.5.2.16 *ISSN: 2349-6495(P) | 2456-1908(O)*

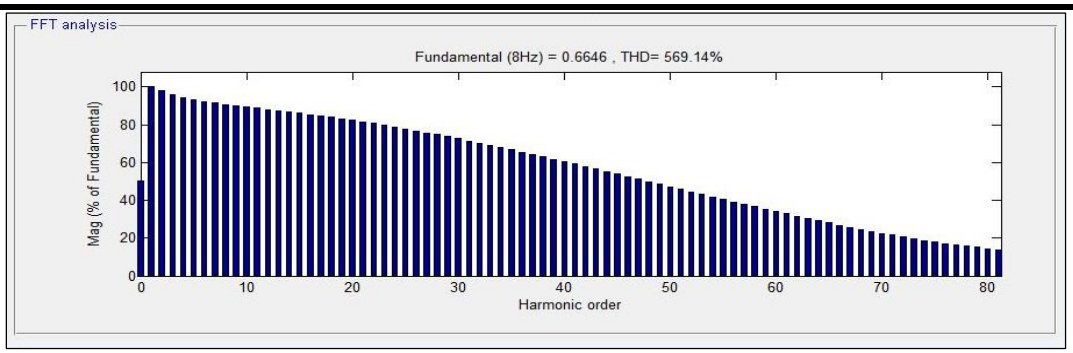

Fig. 19: The frequency spectrum of current for hysteresis control motor at no load.

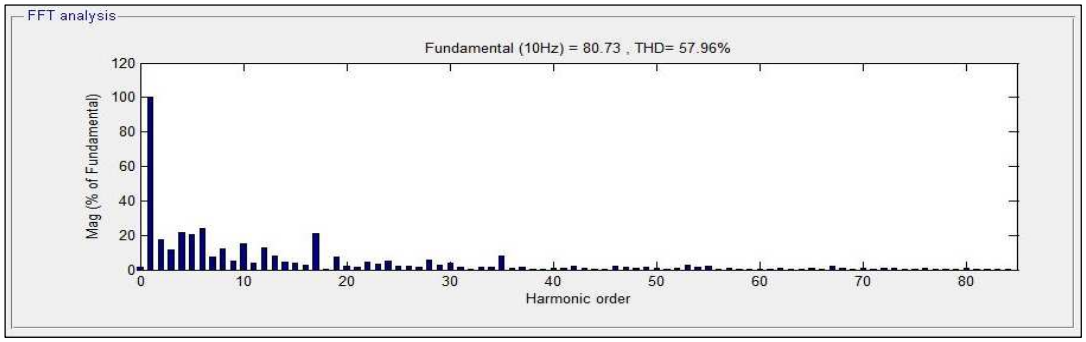

Fig. 20: The frequency spectrum of current for hysteresis control motor at full load.

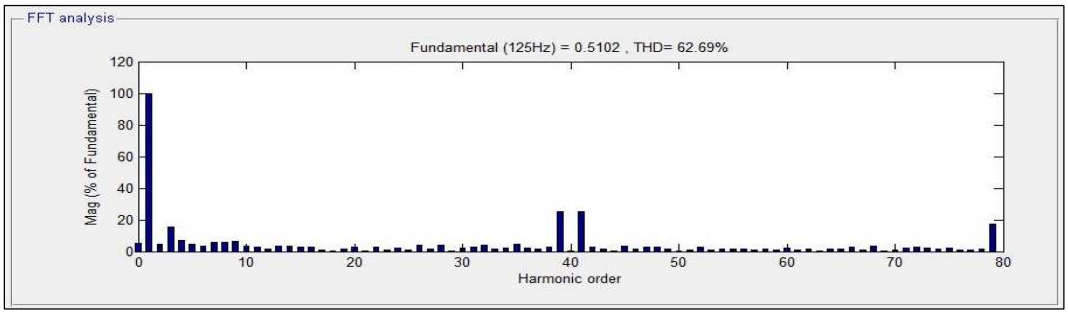

Fig. 21: The frequency spectrum of current for variable dc-link voltage control motor at no load.

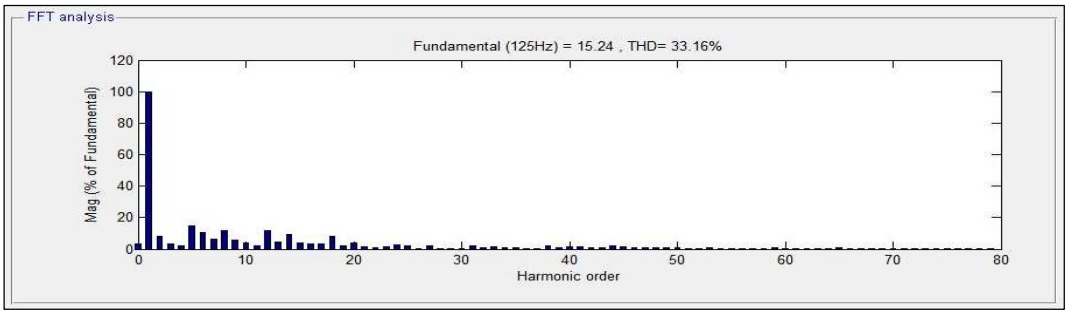

Fig. 22: The frequency spectrum of current for variable dc-link voltage control motor at full load.

https://dx.doi.org/10.22161/ijaers.5.2.16 *ISSN: 2349-6495(P) | 2456-1908(O)*

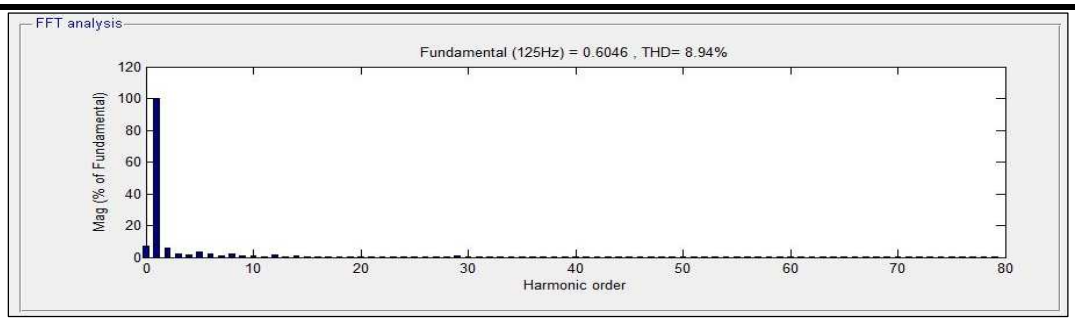

Fig. 23: The frequency spectrum of current for PWM control motor at no load.

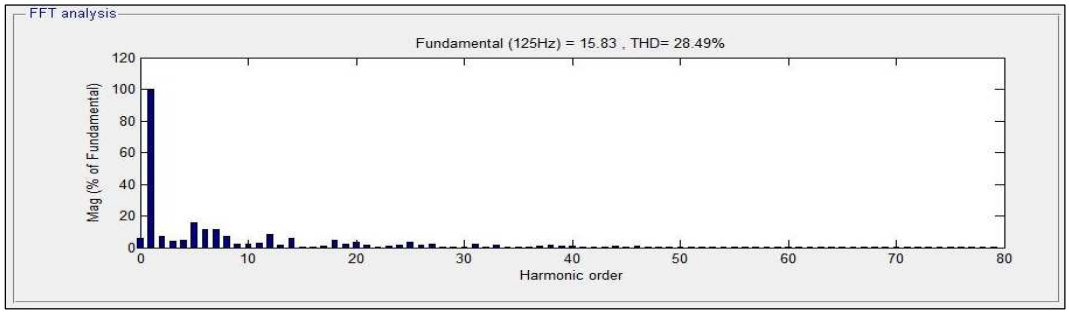

Fig. 24: The frequency spectrum of current for PWM control motor at full load.

VII. COMPARISON BETWEEN CONTROLLING METHODS

The comparison is done with respect to the operation and results from the output waveform of the performing models and the FFT analysis results as shown in Table 4 below:

Table.4: Comparison between controlling methods.

Methods / Subject		Hysteresis band	Variable dc-link	PWM
Signal's ripple		**Very high**	**Medium**	**Low**
Current THD	At no load	569.14%	62.69%	8.94%
	At full load	57.96%	33.16%	28.49%
Applicable		Very easy	Easy	Difficult
Output RMS current A	At no load (0.66) A	0.6646	0.5102	0.6046
	At full load (16) A	80.73	15.24	15.83
Operation frequency		Variable with load (8-10)Hz	Constant with load 125Hz	Constant with load 125Hz

VIII. CONCLUSION

In this paper, the BLDC motor speed and current control was performed using three various control methods: hysteresis band, variable dc-link voltage and PWM speed control methods. All of them are performed well and discussed its drawbacks. The PID parameters are optimized using PSO algorithm which gives optimal values with stable operation. All the mentioned controllers expect the hysteresis controller are attached to the current controller to limit the starting and operation current in order to protect the motor and other connected devices. Frequency analysis was implemented using FFT analysis and found that the hysteresis control has uncontrolled switching frequencies that may be unacceptable in more situations as narrow hysteresis band high switching losses. Because of a fixed frequency in variable dc-link voltage and PWM speed controller makes the most popular in speed control. But the PWM technique is more preferably above two methods.

https://dx.doi.org/10.22161/ijaers.5.2.16 *ISSN: 2349-6495(P) | 2456-1908(O)*

REFERENCES

[1] Chang-liang Xia, Permanent magnet brushless DC motor drives and controls, John Wiley & Sons, First Edition, ISBN 978-1-118-18833-0, (2012).

[2] Stefan B., "BLDC motor modeling and control a Matlab/Simulink implementation", Master Thesis in Electrical Power Engineering, Chalmers University of Technology, Gothenburg, Sweden, (May 2005).

[3] Shivraj S. Dudhe and Archana G. Thosar, "Mathematical modeling andsimulation of three phase BLDC motor using Matlab/Simulink", International Journal of Advances in Engineering & Technology, Vol.7, No.5, pp.1426-1433, (2014).

[4] H. Hao, JianxinShen, Cheng Yuan, and QiangQu,"Influences of machine structure on high speed PM BLDC motor", Electrical Machines and Systems (ICEMS), 17th International Conference on IEEE, 2014.

[5] Mikerov, Alexander G. "Brushless DC torque motors quality level indexes for servo drive applications", EUROCON'09, IEEE, 2009.

[6] Kerdsup, Burin, and Nisai H. Fuengwarodsakul, "Analysis of brushless DC motor in operation with magnetic saturation using FE method", Electrical Engineering/Electronics, Computer, Telecommunica- tionsand Information Technology (ECTI-CON), 8th International Conference on IEEE, 2011.

[7] Md Mustafa Kamal, Lini M. and S. Chatterji, "Speed control of brushlessDC motor using intelligent controllers", IEEE, Students Conference on Engineering and Systems (SCES), PP.1-5, (May 2014).

[8] Wu, Han-Chen, Min-Yi Wen, and Ching-Chang Wong, "Speed control of BLDC motors using hall effect sensors based on DSP", System Science and Engineering (ICSSE), International Conference on IEEE, 2016.

[9] Zhang, Songmao, and Yunliang Wang. "The simulation of BLDC motor speed control based-optimized fuzzy PID algorithm", Mechatronics and Automation (ICMA), International Conference on IEEE, 2016.

[10] Shamseldin, Mohammed Abdelbar, and Adel A. EL-Samahy, "Speed control of BLDC motor by using PID control and self-tuning fuzzy PID controller",Research and Education in Mechatronics (REM), 15th International Workshop on IEEE, 2014.

[11] Adel A.Obed and Ameer L. Saleh,"Speed Control of Brushless DC Motor based on Fractional Order PID Controller", International Journal of Computer Applications 95.4 (2014).

[12] Tibor, Balogh, ViliamFedak, and FrantišekDurovský, "Modeling and simulation of the BLDC motor in MATLAB GUI", Industrial Electronics (ISIE), 2011 IEEE International Symposium on IEEE, 2011.

[13] Kadhim, Abbas K., and Adel A. Obed. "Brushless DC Motor Speed Control Based on PID Controller with 2-DOF and Anti-Windup Techniques."The Second Engineering Conference for Graduate Research, Middle Technical University-Electrical Engineering Technical College Baghdad-Iraq, SECGR 01-01, 2017.

[14] Rambabu S., "Modeling and control of a brushless DC motor", MasterThesis in Power Control and Drives Technology, National Institute of Technology Rourkela, (2007).

[15] Pillay P., Krishnan R., "Modeling, simulation, and analysis of permanentmagnet motor drives, part I: the permanent-magnet synchronous motor drive ", IEEE Transactions on Industry Applications, Vol.2, PP.265-273, (Apr. 1989).

[16] Rodriguez, Fernando, and Ali Emadi. "A novel digital control technique for brushless DC motor drives: Steady state and dynamics." IEEE Industrial Electronics, IECON 2006-32nd Annual Conference on. IEEE, 2006.

[17] Zhou, Xinxiu, and Jiancheng Fang, "Precise braking torque control for attitude control flywheel with small inductance brushless DC motor", IEEE Transactions on Power Electronics 28.11 (2013): 5380-5390.

[18] Texas Instruments Incorporated. DSP Solution for BLDC Motors 1997.

[19] Sue, Shinn-Ming, and Kun-Lin Wu, "A voltage-controlled brushless DCmotor drive over extended speed range", IEEE International Conference on Industrial Technology, ICIT, pp.1-5, (2008).

[20] R. Eberhartand J. Kennedy, "Particle swarm optimization", IEEEInternational Conference on Neural Networks, Perth, Australia, IEEE Service Center, Piscataway, NJ, pp.1942-1948, (1995).

[21] Effatnejad R., Bagheri S., Farsijani M., Talebi R., "Economic Dispatch with Particle Swarm Optimization and Optimal Power Flow", International Journal on "Technical and Physical Problems of Engineering" (IJTPE), Vol. 5, March 2013, PP. 9-16.

[22] Mohammad S. Rahimian and Kaamran R., "Optimal PID Controller Design for AVR System Using Particle Swarm Optimization Algorithm", IEEE, 24th Canadian Conference on Electrical and Computer Engineering (CCECE), May 2011, PP. 337-340.

https://dx.doi.org/10.22161/ijaers.5.2.16 *ISSN: 2349-6495(P) | 2456-1908(O)*

[23] Taeib A., Ltaeif A., Chaari A., "A PSO Approach for Optimum Design of Multivariable PID Controller for Nonlinear Systems", International Conference on Control, Engineering & Information Technology (CEIT'13) Proceedings Engineering & Technology, Vol. 2, 2013, PP. 206-210.

[24] Adel M. Sharaf, Adel A. A. El-Gammal, "A novel particle swarmoptimization PSO tuning scheme for PMDC motor drives controllers", IEEE International Conference on Power Engineering, Energy and Electrical Drives, pp.134-139, (March 2009).

[25] Mehdi N., Hossein N. and Malihe M., "A PSO-based optimum design ofPID controller for a linear brushless dc motor", Procedings of World Academy of Science, Engineering and Technology, Vol.20, PP.211-215, (April 2007).

[26] Anup Kumar Panda and Sushree Sangita Patnaik, "Analysis of cascaded multilevel inverters for active harmonic filtering in distribution networks", International Journal of Electrical Power &Energy Systems, Vol.66, pp.216- 226, (2015).

[27] Power Factor Correction, "A Guide for the Plant Engineer", Technical data SA02607001E (2010).